대한영상의학회지

Usefulness of Tissue Permeability Factor in Differentiating Benign and Malignant Pulmonary Lesions on Dynamic Contrast-Enhanced MRI[1]
악성과 양성 폐병변의 감별에 있어 역동적 자기공명영상 조직 투과 인자의 유용성[1]

Sung Hyun Baik, MD[1], Gong Yong Jin, MD[1,2], Young Min Han, MD[1,2], Yong Chul Lee, MD[3], Keun Sang Kwon, MD[4]

[1]Department of Radiology, Chonbuk National University Hospital, Jeonju, Korea
Departments of [2]Radiology, [3]Internal Medicine, [4]Preventive Medicine, Chonbuk National University Medical School and Hospital, Research Institute of Clinical Medicine, Jeonju, Korea

Purpose: To evaluate the clinical usefulness of tissue permeability factor in differentiating benign and malignant pulmonary lesions on dynamic contrast-enhanced (DCE) MRI.

Materials and Methods: 30 patients (14 women, 16 men; median age, 64 years; age range, 41-80 years) who had a pulmonary lesion underwent DCE MR imaging at 3.0 T. Fifteen patients had lung cancer and 15 patients had benign pulmonary nodules. To calculate the perfusion parameters of the pulmonary lesions, quantitative analysis was carried out on all 30 pulmonary nodules or masses: volume transfer constant (K^{trans}), reflux constant (K_{ep}), and extravascular extracellular space volume fraction (v_e). A Mann-Whitney test was used to calculate the statistical significance of quantitative perfusion parameters between malignant and benign pulmonary lesions. Receiver operating characteristic curve analysis was also performed for evaluation of sensitivity and specificity of perfusion parameters to diagnose lung cancer.

Results: Malignant pulmonary lesions had higher K^{trans} and v_e values than benign pulmonary lesions (0.227 ± 0.065 vs. 0.133 ± 0.054; $p = 0.001$, 0.479 ± 0.156 vs. 0.357 ± 0.13; $p = 0.038$, respectively). However, the difference in K_{ep} between the benign and malignant pulmonary lesion was not significant (0.648 ± 0.44 vs. 0.797 ± 0.93; $p = 0.709$). With a threshold of 0.202 (min^{-1}), the sensitivity and specificity to diagnose malignant pulmonary lesions of the K^{trans} value were 66.6% and 93.3%, respectively.

Conclusion: K^{trans} and v_e value of perfusion parameters on DCE-MRI can help to discriminate between malignant and benign pulmonary nodules or masses.

INTRODUCTION

Quantitative techniques including fluorodeoxyglucose positron emission tomography, perfusion CT, and dynamic contrast material enhanced magnetic resonance imaging (DCE-MRI) have recently been used for differentiating benign and malignant lesions (1-5). Among these, DCE-MRI was able to assess endo-thelial volume transfer, providing information about pharmacokinetic parameters such as volume transfer constant (K^{trans}), the rate constant that represents transfer of the contrast agent from the extravascular extracelluar space (EES) to the blood plasma (K_{ep}), and extravascular extracellular volume fraction (v_e) (3-5). Using these parameters, DCE-MRI has been used in the diagnosis and management of many oncological cases, including

breast, bone, abdomen, and hematologic cancers (6-10).

However, it is still not easy to apply DCE-MRI to pulmonary lesions due to motion artifacts caused by respiration, cardiac pulsation, relatively low spatial resolution, and low reproducibility. Recently, studies have been reported that compare malignant and benign lung lesions from the enhancement pattern of DCE-MRI using kinetic and morphologic parameters (11-14). To the best of our knowledge, however, no study has been conducted that differentiates benign from malignant pulmonary lesions using quantitative perfusion parameters.

The purpose of our study was therefore to determine whether tissue permeability factor (K^{trans}, K_{ep}, or v_e) on DCE-MRI can help to discriminate between malignant and benign pulmonary nodules or masses.

MATERIALS AND METHODS

Patient

A total of 43 consecutive patients with diagnosis of pulmonary nodules or masses underwent DCE-MRI from June 2010 to May 2011. All data were retrospectively reviewed and the study received institutional review board approval. However, informed consent was not waived for all patients. Inclusion criteria were as follows: 1) pulmonary nodule or mass sizes between 1 cm and 5 cm on chest CT regardless of enhancement; 2) pulmonary nodules or masses had been pathologically proven using biopsy after patients underwent MRI; 3) subjects had not undergone radiation therapy or chemotherapy previously if they had been diagnosed with lung cancer. Subsequently, 11 patients were excluded from analysis because their pulmonary lesions were unable to be detected correctly on dynamic contrast-enhanced MR images due to combined pneumonia or atelectasis. Two patients were excluded from post-processing analysis owing to substantial motion artifact. Finally, the remaining 30 patients (14 women, 16 men; median age, 64 years; age range, 41-80 years) were included in this study. Among the 30 nodules or masses, 15 were benign, including chronic granulomatous inflammation with/without necrosis ($n = 7$), nonspecific chronic inflammation ($n = 4$), organizing pneumonia ($n = 2$), and fibrotic nodule ($n = 2$). Fifteen cases of malignancy were detected, including adenocarcinoma ($n = 9$, mean size: 32.8 ± 1.25 mm) and squamous cell carcinoma ($n = 6$, mean size: 40 ± 1.05 mm).

All 30 pulmonary nodules or masses were histologically proven by percutaneous transthoracic needle biopsies ($n = 28$) and transbronchial lung biopsies ($n = 2$). Biopsies were routinely performed before initiating the appropriate therapy. In addition, 5 patients subsequently underwent lung resection.

MR Protocol

All patients underwent MR imaging, which was performed with a 3.0-T (Magnetom Verio, Siemens Healthcare, Erlangen, Germany) in the supine position. A six-channel phased-array body coil with parallel imaging capability was placed over the thorax to reduce susceptibility artifacts and improve imaging quality. Initially, scout images were obtained using turbo-inversion recovery with a coronal plane. Subsequently, pre-contrast three-dimensional (3D) T1-weighted volumetric interpolated breath-hold examination (VIBE) sequences using different flip angles (2° and 15°) were obtained for anatomic images. All images were obtained in the transverse plane. The MRI scanning range was applied differently in each case to include the entire tumor within a volume of section. After the pre-contrast phase was completed, DCE-MRI was performed using a 3D T1-weighted VIBE sequence with a 15° flip angle (repetition time/echo time: 3.78/1.28, flip angle: 15°, matrix: 184 × 256, field of view: 350 × 350, slice thickness: 5 mm, slice per slab: 30, bandwidth: 450 Hz/pixel, NEX: 1, scan time: 4 min 57 s). Thirty-five dynamic measurements were performed. The acquisition time was 8.5 seconds with a single dynamic measurement. After the first three measurements, an intravenous bolus of 0.1 mmol gadobutrol (gadolinium-DO3A-butriol, Gadovist 1.0; Bayer HealthCare, Berlin, Germany) per kilogram of body weight was injected at amounts of 10 cc at 3 mL/sec using a power injector (Spectris®; Medrad, Pittsburgh, PA, USA). DCE-MRI obtained the repeated acquisition of a VIBE sequence before, during, and after a contrast agent.

Image Analysis and Statistical Analysis

Post-processing of all DCE-MRI data was performed by using a commercial software tool (Tissue 4D; Siemens Healthcare, Erlangen, Germany). Initially, motion correction was carried out automatically, after which we registered morphological and pre-contrast data to the dynamic series using software (Tissue 4D; Siemens Healthcare, Erlangen, Germany). A value for the arteri-

al input function was automatically calculated using the software without an arterial region of interest (ROI). After obtaining a kinetic modeling parameter map, ROI was drawn on the post-contrast subtracting image. The ROIs were drawn along the contours of each pulmonary nodule to encompass the entire tumor; this was performed by a radiologist who was blind to the patient history with care taken to exclude areas of artifact and blood vessels. One month later, the same radiologist again drew the ROIs along contours of pulmonary nodules to obtain the average value of parameters. Three parameters, K^{trans}, v_e, and K_{ep} were automatically calculated from the fitted model and concentration curve. Finally, the means of these parameters of pixels within the drawn regions of interest were recorded for all patients. K^{trans} is the volume transfer constant that represents the transfer of contrast agent between the blood plasma and the EES (min^{-1}). K_{ep} is the rate constant that represents transfer of the contrast agent from the EES to the blood plasma (in min^{-1}), and v_e = K^{trans} / K_{ep} is the volume of EES per unit volume of tissue (5).

Statistical analysis was performed using a Graphpad prism, version 5.0 (GraphPad Software, San Diego, CA, USA). A Mann-Whitney test was used to compare the age, sex, size, location, and distribution of benign lesions with malignant lesions. A Mann-Whitney test was also used to calculate the statistical significance

of quantitative perfusion parameters as follows: upper lobe vs. middle/lower lobe, central vs. peripheral, size (less than 30 mm, more than 30 mm), and benign vs. malignant nodules or masses. Receiver operating characteristic analysis was also performed for the evaluation of the sensitivity and specificity of perfusion parameters for diagnosis of malignancy. $p < 0.05$ was considered to be statistically significant.

RESULTS

The characteristics of our patients are shown in Table 1. No significant difference occurred in sex, location, or distribution between benign and malignant pulmonary lesions. However, the age and size of lesion of the malignant group were significantly greater than those of the benign group ($p = 0.032$ and 0.005, respectively).

Table 2 and 3 show the quantitative perfusion parameters for the location and size of pulmonary lesions regardless of benignancy and malignancy. No significant difference of quantitative perfusion parameters occurred for the location and size of pulmonary lesions, regardless of the presence of malignancy. Table 4 shows the quantitative perfusion parameters between benignancy and malignancy of lesions regardless of size. Among the

Table 1. Patient Characteristics in Our Study: Benignancy vs. Malignancy

	Benignancy (*n* = 15)	Malignancy (*n* = 15)	*p* Value
Age (years)	60.3	68.5	0.032
Sex (male : female)	10 : 5	6 : 9	0.157
Size (mm)	22.4	35.6	0.005
Location			0.735
Upper	8 (26.6)	9 (30)	
Middle	2 (6.6)	1 (3.3)	
Lower	5 (16.6)	5 (16.6)	
Distribution			0.149
Central	7 (23.3)	11 (36.6)	
Peripheral	8 (26.6)	4 (13.3)	

Note.─Data in parentheses are percentages. *p* value < 0.05 is statistically significant.

Table 2. Comparison of Quantitative Perfusion Parameter for Location of Lesions (*n* = 30) Regardless of Benignancy and Malignancy

Parameter	Location					
	Upper (*n* = 17)	Middle/Lower (*n* = 13)	*p* Value	Central (*n* = 12)	Peripheral (*n* = 18)	*p* Value
K^{trans}	0.182 ± 0.08	0.177 ± 0.078	0.769	0.18 ± 0.058	0.18 ± 0.087	0.949
K_{ep}	0.862 ± 0.884	0.539 ± 0.379	0.072	0.588 ± 0.228	0.812 ± 0.909	0.783
v_e	0.366 ± 0.117	0.485 ± 0.174	0.066	0.433 ± 0.13	0.407 ± 0.171	0.512

Note.─Data are means ± standard deviation. Mann-Whitney test was used. K^{trans} means forward volume transfer constant. K_{ep} means reverse reflux rate constant between extracellular space and plasma. v_e means extravascular extracellular volume fraction. *p* value < 0.05 is statistically significant.

three perfusion parameters, the K^{trans} and v_e values showed a significant difference. The mean K^{trans} and v_e values of malignant lesions were significantly higher than those of benign lesions (0.227 ± 0.065 vs. 0.133 ± 0.054; $p = 0.001$, 0.479 ± 0.156 vs. 0.357 ± 0.13; $p = 0.038$, respectively) (Figs. 1, 2). However, the difference in K_{ep} between the two groups was not significant. With a K^{trans} value threshold of 0.202 (min^{-1}), the sensitivity and specificity of K^{trans} value were 66.6% and 93.3%, respectively, for

Table 3. Comparison of Quantitative Perfusion Parameter for Size of Lesions Regardless of Benignancy and Malignancy

Parameter	Size (mm)		
	≤ 30 (n = 14)	> 30 (n = 16)	p Value
K^{trans}	0.165 ± 0.056	0.193 ± 0.089	0.394
K_{ep}	0.615 ± 0.391	0.817 ± 0.092	0.603
v_e	0.411 ± 0.146	0.423 ± 0.16	0.787

Note.—Data are means ± standard deviation. Mann-Whitney test was used. K^{trans} means forward volume transfer constant. K_{ep} means reverse reflux rate constant between extracellular space and plasma. v_e means extravascular extracellular volume fraction. p value < 0.05 is statistically significant.

Table 4. Comparison of Quantitative Perfusion Parameter between Benignancy and Malignancy Regardless of Lesion Size

Parameter	Final Diagnosis		
	Benignancy (n = 15)	Malignancy (n = 15)	p Value
K^{trans}	0.133 ± 0.054	0.227 ± 0.065	0.001
K_{ep}	0.648 ± 0.44	0.797 ± 0.93	0.709
v_e	0.357 ± 0.13	0.479 ± 0.156	0.038

Note.—Data are means ± standard deviation. Mann-Whitney test was used. K^{trans} means forward volume transfer constant. K_{ep} means reverse reflux rate constant between extracellular space and plasma. v_e means extravascular extracellular volume fraction. p value < 0.05 is statistically significant.

differentiating malignant from benign pulmonary lesions. Meanwhile, the sensitivity and specificity of K^{trans} value at a threshold of 0.158 (min^{-1}) were 93.3% and 66.6%, respectively, for predicting malignancy. To produce a specificity of 100% while we maximized sensitivity, the optimal K^{trans} threshold values for the prediction of differentiation of malignant pulmonary lesion from benign lesion was greater than 0.23 (min^{-1}).

Table 5 shows the quantitative perfusion parameters between benign lesions and malignant lesions according to size. In lesion size of less than 30 mm, no significant difference of perfusion parameters was detected between benign and malignant lesions. Meanwhile, in lesion size of more than 30 mm, only the K^{trans} values of malignant pulmonary lesions were significantly higher than the benign lesions (0.233 ± 0.07 vs. 0.104 ± 0.054; $p = 0.007$) (Figs. 3, 4).

Among malignant lesions, no significant difference of perfusion parameters between squamous cell carcinomas and adenocarcinomas was detected (mean K^{trans}; 0.256 ± 0.076 vs. 0.208 ± 0.052, mean K_{ep}; 1.183 ± 1.431 vs. 0.54 ± 0.221 mean v_e; 0.451 ± 0.172 vs. 0.497 ± 0.152).

DISCUSSION

Recently, quantitative perfusion parameters using DCE-MRI are emerging as potential methods for differentiating benign from malignant lesions (15-20). Many investigators have suggested that K^{trans} measured using DCE-MRI shows relatively high sensitivity and specificity for differentiating normal from
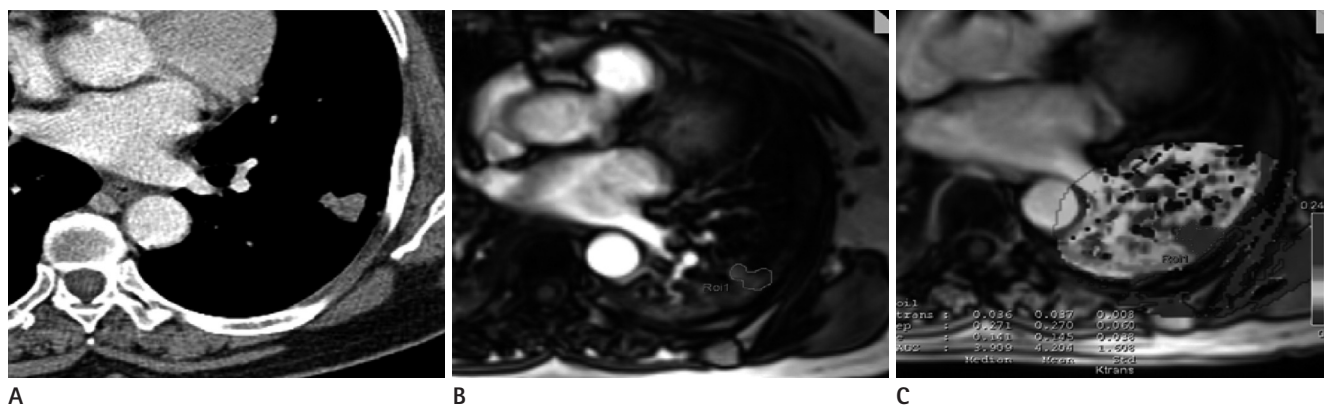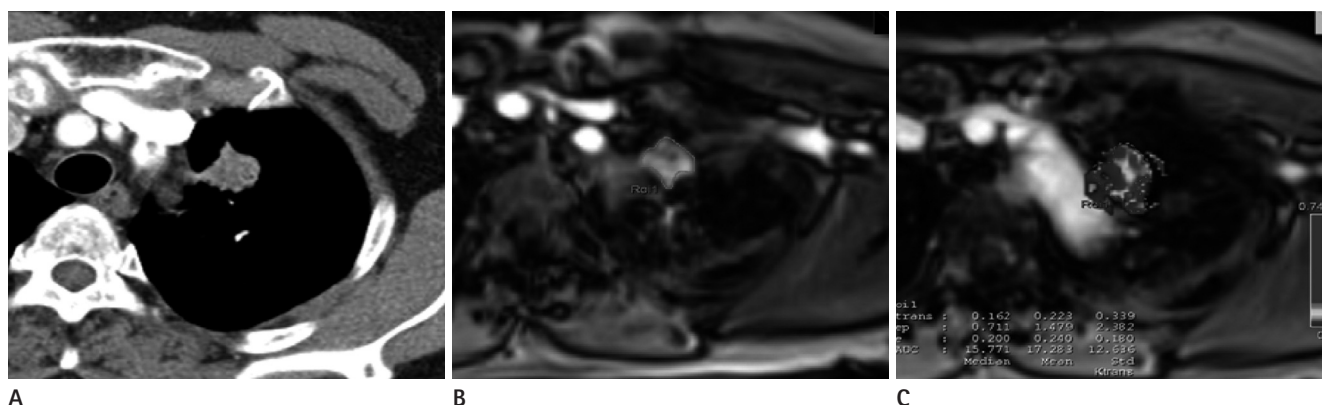

Fig. 1. A 63-year-old woman with pulmonary cryptococcosis.
A. Chest CT shows solitary pulmonary nodule (SPN) in peripheral portion of left lower lobe (1.8 cm).
B. Region of interest is drawn along contour of lesion manually on contrast-enhanced T1-weighted axial image.
C. Corresponding parametric map of perfusion obtained by Tissue 4D software using two-compartment kinetic model shows low permeability in SPN (mean K^{trans} value = 0.037 min^{-1}).

Fig. 2. A 61-year-old woman with lung malignancy (adenocarcinoma).
A. Chest CT shows solitary pulmonary nodule (SPN) in central of left upper lobe (2 cm).
B. Region of interest is drawn along contour of lesion manually on contrast-enhanced T1-weighted axial image.
C. Corresponding parametric map of perfusion for the SPN shows heterogeneous high permeability within tumor (mean K^{trans} value = 0.223 min^{-1}).
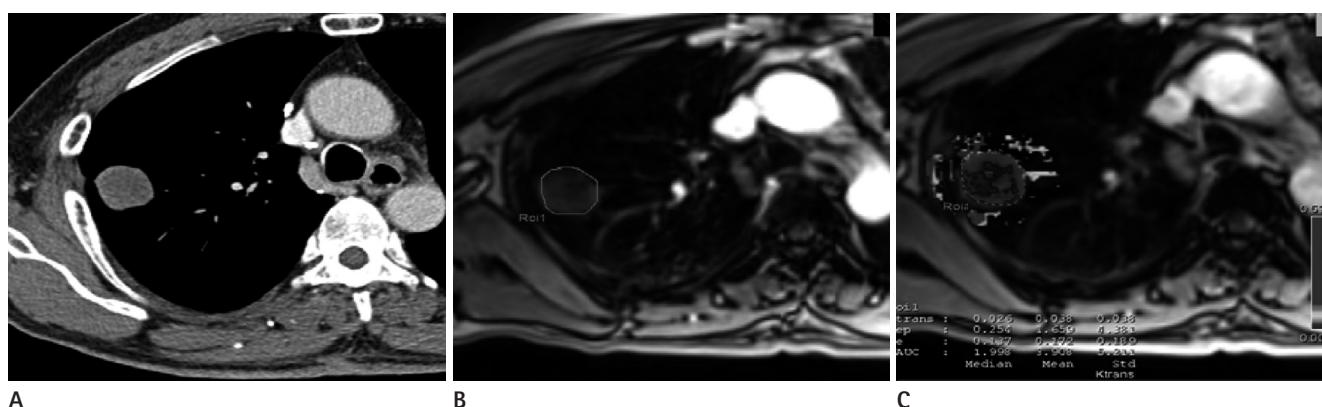
Fig. 3. A 56-year-old man with pulmonary tuberculosis.
A. Chest CT shows solitary pulmonary nodule (SPN) in peripheral portion of right upper lobe (3.3 cm).
B. Region of interest is drawn along contour of lesion manually on contrast-enhanced T1-weighted axial image.
C. Corresponding parametric map of perfusion of the SPN shows homogeneous low permeability (mean K^{trans} value = 0.038 min^{-1}).

**Table 5. Comparison of Quantitative Perfusion Parameter between Benignancy and Malignancy by Size of Lesions**

Parameter	Size (mm)					
	≤ 30 (n = 14)			> 30 (n = 16)		
	Benignancy (n = 10)	Malignancy (n = 4)	p Value	Benignancy (n = 5)	Malignancy (n = 11)	p Value
K^{trans}	0.148 ± 0.05	0.21 ± 0.054	0.106	0.104 ± 0.054	0.233 ± 0.07	0.007
K_{ep}	0.559 ± 0.413	0.755 ± 0.339	0.304	0.827 ± 0.485	0.812 ± 1.085	0.257
v_e	0.387 ± 0.131	0.475 ± 0.184	0.454	0.297 ± 0.118	0.48 ± 0.155	0.054

Note.—Data are means ± standard deviation. Mann-Whitney test was used. K^{trans} means forward volume transfer constant. K_{ep} means reverse reflux rate constant between extracellular space and plasma. v_e means extravascular extracellular volume fraction. p value < 0.05 is statistically significant.

cancerous tissue in colorectal and prostate cancer in selected patients (21-23). Similar to these results, our study demonstrated a significant difference in K^{trans} value between benign and malignant pulmonary nodules or masses measured using DCE-MRI. Considering that K^{trans} is positively coupled to blood flow, endothelial permeability and surface area, high K^{trans} values imply an increased vascular permeability with disease progression such

as malignant status (24). Meanwhile, Ng et al. (25) suggested that tumor size is not a significant variable for K^{trans}, at least in the range of tumor size; that is, 2.5-9.3 cm. However, in our study, we found that K^{trans} was affected by the size of the pulmonary lesion. In K^{trans} values of lesions more than 30 mm in size, a statistically significant difference occurred between benign and malignant pulmonary nodules. This might be explained by the
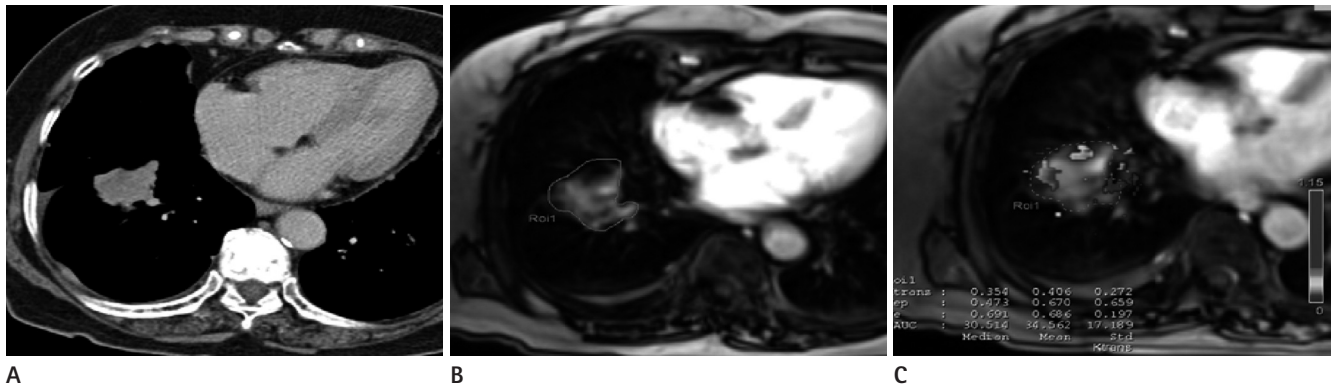
Fig. 4. A 81-year-old woman with lung malignancy (adenocarcinoma).
A. Chest CT shows a lobular shaped mass in peripheral of right lower lobe (4 cm).
B. Region of interest is drawn along contour of lesion manually on contrast-enhanced T1-weighted axial image.
C. Corresponding parametric map of perfusion for the pulmonary mass shows high permeability within tumor (mean K^{trans} value = 0.406 min^{-1}).

relative paucity of the functional blood vessels in small tumors, even if highly permeable. In addition, our results show no significant difference of perfusion parameters between squamous cell carcinomas and adenocarcinomas. The high K^{trans} values of both malignant groups might be explained by the mean size of lesions of over 30 mm for both malignant groups.

In adenocarcinoma, the poorly represented microvascular component could be explained by the functional impairment of the vessel, incompletely formed, and by the presence of a prominent stromal matrix that embeds the vessels (26). This could also explain why small malignant pulmonary nodules have relatively low K^{trans} values. Thus, we suspect that perfusion parameter values would be compromised with smaller pulmonary lesions. Our study shows that the K^{trans} value was a useful parameter for discriminating malignant from benign pulmonary lesions. The K^{trans} threshold value of more than 0.23 (min^{-1}) shows 100% specificity for the differentiation of malignant from benign pulmonary lesions.

The range of K^{trans} values of malignant pulmonary nodules or masses in our study is 0.16-0.39 min^{-1} (mean value = 0.227 ± 0.065 min^{-1}). Our results differ from those of prior studies. Ng et al. (25) reported K^{trans} values for liver and lung tumors in the range of 0.028-0.16 min^{-1}. Galbraith et al. (27) reported K^{trans} values for a variety of tumors in the range 0.07-1.03 min^{-1}. K^{trans} values for a variety of tumors are influenced by various factors such as permeability of vascular surface area, contrast of concentration in the vessel as well as vascular density, blood flow, and cardiac output (28). In our study, the high osmolar MR contrast was twice that of the high K^{trans} in malignant nodules or masses than Ng et al. (25). We then demonstrated that the mean value of K^{trans} in malignant nodules or masses can be affected by MR contrast concentration.

Another quantitative parameter, v_e, representing the volume fraction of the contrast agent in the extravascular extracellular space, increases in proportion to capillary leakage (29). Much attention has been given to the change of v_e before and after treatment; recently, v_e has been regarded as a prognostic parameter for the outcome of cancer treatment, especially chemotherapy or radiotherapy (30). However, discrepancies between studies remain. A study of prostate cancers showed that no significant difference was shown in perfusion parameters (v_e) between prostate tumors and benign inflammations (31). Furthermore, some overlaps still appear to exist in the enhancement patterns between tumors and benign areas of the peripheral zone such as those affected by prostatitis, post-biopsy hemorrhage, and benign prostatic hyperplasia (31). In our study, however, a marginally significant difference was detected in the v_e value between benign and malignant pulmonary lesions of more than 30 mm size. In pulmonary lesions less than 30 mm in size, no significant difference of v_e value was detected between benign lesions and malignant lesions. This might be due to tumor angiogenesis, characterized structurally by abnormal blood vessels lacking the vessel hierarchy and having a heterogeneous distribution, while the extravascular extracellular space could vary according to lesion size (24). These results suggest that v_e values may not be important biomarkers to discriminate benign and malignant pulmonary nodules or masses.

Our study also suggests that tumor location in the lung was

not a significant variable for all three perfusion parameters, regardless of benignancy and malignancy. This suggests that perfusion parameters may not be influenced by location or zonal distribution of lesions, but of course must exclude other abnormalities such as pneumonia. However, this speculation will need further experimental studies for confirmation.

Our study has several limitations. First, we did not fully exclude tumor necrosis in the selection of ROIs and we did not consider hotspot areas in the tumors. Thus, the quantitative parameters from the axial T1 weighted MR imaging might not reflect the tumors' real burden. Second, the total number of pulmonary lesions studied was relatively small. In particular, the numbers of pulmonary lesions according to size may be too small to perform reliable comparisons of the subgroup of benign and malignant lesions presented here. As such, a further study with a larger patient group and a more extensive histological type should be performed to appraise the diagnostic value of DCE-MRI in pulmonary lesions. Thirdly, the within-patient coefficients of variation for K^{trans} for lung lesions was known to be about 20% because of MRI susceptibility artifacts, vascular pulsation artifacts, and difficulty in delineating tumor margins (25). Because we did not assess the intra-individual variability of pharmacokinetic parameters in our patient population, our data might not be widely accepted due to decreased confidence.

In conclusion, our study shows that the K^{trans} values of malignant pulmonary lesions are higher than those of benign pulmonary lesions, and that the optimal value of K^{trans} shows high sensitivity and specificity for pulmonary malignant nodules or masses. Thus, the K^{trans} value of perfusion parameters on DCE-MRI can help to discriminate between benign and malignant pulmonary nodules or masses.

REFERENCES

1. Gould MK, Maclean CC, Kuschner WG, Rydzak CE, Owens DK. Accuracy of positron emission tomography for diagnosis of pulmonary nodules and mass lesions: a meta-analysis. *JAMA* 2001;285:914-924

2. Ohno Y, Koyama H, Matsumoto K, Onishi Y, Takenaka D, Fujisawa Y, et al. Differentiation of malignant and benign pulmonary nodules with quantitative first-pass 320-detector row perfusion CT versus FDG PET/CT. *Radiology* 2011;258: 599-609

3. Oostendorp M, Post MJ, Backes WH. Vessel growth and function: depiction with contrast-enhanced MR imaging. *Radiology* 2009;251:317-335

4. Tofts PS. Modeling tracer kinetics in dynamic Gd-DTPA MR imaging. *J Magn Reson Imaging* 1997;7:91-101

5. Tofts PS, Brix G, Buckley DL, Evelhoch JL, Henderson E, Knopp MV, et al. Estimating kinetic parameters from dynamic contrast-enhanced T(1)-weighted MRI of a diffusable tracer: standardized quantities and symbols. *J Magn Reson Imaging* 1999;10:223-232

6. O'Connor JP, Jackson A, Asselin MC, Buckley DL, Parker GJ, Jayson GC. Quantitative imaging biomarkers in the clinical development of targeted therapeutics: current and future perspectives. *Lancet Oncol* 2008;9:766-776

7. Marcus CD, Ladam-Marcus V, Cucu C, Bouché O, Lucas L, Hoeffel C. Imaging techniques to evaluate the response to treatment in oncology: current standards and perspectives. *Crit Rev Oncol Hematol* 2009;72:217-238

8. Akisik MF, Sandrasegaran K, Bu G, Lin C, Hutchins GD, Chiorean EG. Pancreatic cancer: utility of dynamic contrast-enhanced MR imaging in assessment of antiangiogenic therapy. *Radiology* 2010;256:441-449

9. Padhani AR. Dynamic contrast-enhanced MRI in clinical oncology: current status and future directions. *J Magn Reson Imaging* 2002;16:407-422

10. Padhani AR, Hayes C, Assersohn L, Powles T, Makris A, Suckling J, et al. Prediction of clinicopathologic response of breast cancer to primary chemotherapy at contrast-enhanced MR imaging: initial clinical results. *Radiology* 2006; 239:361-374

11. Kono R, Fujimoto K, Terasaki H, Müller NL, Kato S, Sadohara J, et al. Dynamic MRI of solitary pulmonary nodules: comparison of enhancement patterns of malignant and benign small peripheral lung lesions. *AJR Am J Roentgenol* 2007;188:26-36

12. Pauls S, Mottaghy FM, Schmidt SA, Krüger S, Möller P, Brambs HJ, et al. Evaluation of lung tumor perfusion by dynamic contrast-enhanced MRI. *Magn Reson Imaging* 2008;26:1334-1341

13. Schaefer JF, Vollmar J, Schick F, Vonthein R, Seemann MD, Aebert H, et al. Solitary pulmonary nodules: dynamic con-

trast-enhanced MR imaging--perfusion differences in malignant and benign lesions. *Radiology* 2004;232:544-553

14. Pauls S, Breining T, Muche R, Schmidt SA, Wunderlich A, Krüger S, et al. The role of dynamic, contrast-enhanced MRI in differentiating lung tumor subtypes. *Clin Imaging* 2011;35:259-265

15. Kaiser WA, Zeitler E. MR imaging of the breast: fast imaging sequences with and without Gd-DTPA. Preliminary observations. *Radiology* 1989;170(3 Pt 1):681-686

16. van der Woude HJ, Verstraete KL, Hogendoorn PC, Taminiau AH, Hermans J, Bloem JL. Musculoskeletal tumors: does fast dynamic contrast-enhanced subtraction MR imaging contribute to the characterization? *Radiology* 1998; 208:821-828

17. Barentsz JO, Engelbrecht M, Jager GJ, Witjes JA, de LaRosette J, van Der Sanden BP, et al. Fast dynamic gadolinium-enhanced MR imaging of urinary bladder and prostate cancer. *J Magn Reson Imaging* 1999;10:295-304

18. Jager GJ, Ruijter ET, van de Kaa CA, de la Rosette JJ, Oosterhof GO, Thornbury JR, et al. Local staging of prostate cancer with endorectal MR imaging: correlation with histopathology. *AJR Am J Roentgenol* 1996;166:845-852

19. Liney GP, Turnbull LW, Knowles AJ. In vivo magnetic resonance spectroscopy and dynamic contrast enhanced imaging of the prostate gland. *NMR Biomed* 1999;12:39-44

20. Williams TC, DeMartini WB, Partridge SC, Peacock S, Lehman CD. Breast MR imaging: computer-aided evaluation program for discriminating benign from malignant lesions. *Radiology* 2007;244:94-103

21. Bloch BN, Lenkinski RE, Rofsky NM. The role of magnetic resonance imaging (MRI) in prostate cancer imaging and staging at 1.5 and 3 Tesla: the Beth Israel Deaconess Medical Center (BIDMC) approach. *Cancer Biomark* 2008;4: 251-262

22. George ML, Dzik-Jurasz AS, Padhani AR, Brown G, Tait DM, Eccles SA, et al. Non-invasive methods of assessing angiogenesis and their value in predicting response to treatment in colorectal cancer. *Br J Surg* 2001;88:1628-1636

23. Jager GJ, Ruijter ET, van de Kaa CA, de la Rosette JJ, Oosterhof GO, Thornbury JR, et al. Dynamic TurboFLASH subtrac-

tion technique for contrast-enhanced MR imaging of the prostate: correlation with histopathologic results. *Radiology* 1997;203:645-652

24. Yao WW, Zhang H, Ding B, Fu T, Jia H, Pang L, et al. Rectal cancer: 3D dynamic contrast-enhanced MRI; correlation with microvascular density and clinicopathological features. *Radiol Med* 2011;116:366-374

25. Ng CS, Raunig DL, Jackson EF, Ashton EA, Kelcz F, Kim KB, et al. Reproducibility of perfusion parameters in dynamic contrast-enhanced MRI of lung and liver tumors: effect on estimates of patient sample size in clinical trials and on individual patient responses. *AJR Am J Roentgenol* 2010;194: W134-W140

26. Bali MA, Metens T, Denolin V, Delhaye M, Demetter P, Closset J, et al. Tumoral and nontumoral pancreas: correlation between quantitative dynamic contrast-enhanced MR imaging and histopathologic parameters. *Radiology* 2011;261:456-466

27. Galbraith SM, Lodge MA, Taylor NJ, Rustin GJ, Bentzen S, Stirling JJ, et al. Reproducibility of dynamic contrast-enhanced MRI in human muscle and tumours: comparison of quantitative and semi-quantitative analysis. *NMR Biomed* 2002;15:132-142

28. Aerts HJ, van Riel NA, Backes WH. System identification theory in pharmacokinetic modeling of dynamic contrast-enhanced MRI: influence of contrast injection. *Magn Reson Med* 2008;59:1111-1119

29. Yu CW, Shih TT, Hsu CY, Lin LC, Wei SY, Lee CM, et al. Correlation between pancreatic microcirculation and type 2 diabetes in patients with coronary artery disease: dynamic contrast-enhanced MR imaging. *Radiology* 2009;252:704-711

30. Kim H, Folks KD, Guo L, Stockard CR, Fineberg NS, Grizzle WE, et al. DCE-MRI detects early vascular response in breast tumor xenografts following anti-DR5 therapy. *Mol Imaging Biol* 2011;13:94-103

31. Ocak I, Bernardo M, Metzger G, Barrett T, Pinto P, Albert PS, et al. Dynamic contrast-enhanced MRI of prostate cancer at 3 T: a study of pharmacokinetic parameters. *AJR Am J Roentgenol* 2007;189:192-201

악성과 양성 폐병변의 감별에 있어 역동적 자기공명영상 조직 투과 인자의 유용성[1]

백성현[1] · 진공용[1,2] · 한영민[1,2] · 이용철[3] · 권근상[4]

목적: 역동적 조영증강 자기공명영상의 투과 인자가 양성과 악성 폐병변 감별에 임상적 유용성이 있는지 알아보고자 하였다.

대상과 방법: 2010년 6월에서 2011년 5월에 걸쳐 폐암이 의심되어 역동적 조영증강 자기공명영상을 촬영한 환자 30명 (여자 14명, 남자 16명, 평균나이 64세, 나이 분포 41~80세)을 대상으로 하였다. 이 중 15명의 환자들은 폐암으로 나머지 15명은 양성 폐결절 또는 종괴로 진단 받았다. 30개의 폐병변에 대해 부피 이동 상수(K^{trans}), 혈관외 세포외 공간 부피 분율(v_e)과 유출 비율 상수(K_{ep})의 관류 지표를 구하였으며, Mann-Whitney test를 이용하여 악성과 양성 폐병변의 정량적 관류 지표들의 통계학적 차이를 알아보았다. 또한 receiver operating characteristic curve를 이용하여 관류 지표들의 악성 폐병변 예측에 민감도와 특이도를 구하였다.

결과: 악성은 양성보다 높은 K^{trans}와 v_e 값을 보였다(0.227 ± 0.065 vs. 0.133 ± 0.054; $p = 0.001$, 0.479 ± 0.156 vs. 0.357 ± 0.13; $p = 0.038$, 각각). 하지만 양성과 악성 폐병변에서 K_{ep} 값은 의미 있는 차이를 보이지 않았다(0.648 ± 0.44 vs. 0.797 ± 0.93; $p = 0.709$). K^{trans}의 값을 $0.202(min^{-1})$로 정했을 때 폐암을 진단하기 위한 민감도와 특이도는 각각 66.6%와 93.3%였다.

결론: 역동적 조영증강 자기공명영상의 관류 지표 중 K^{trans}와 v_e는 악성과 양성 폐병변 감별에 도움이 된다.

[1]전북대학교병원 영상의학과, 전북대학교 의학전문대학원 전북대학교병원 임상의학연구소 [2]영상의학과, [3]호흡기알레르기내과, [4]예방의학과